

## Comparison of the performance of synthesized nano-structure hydroxyapatite with bovine bones and alanine samples for EPR dosimetry

N. Hajiloo<sup>1</sup>, F. Ziaie<sup>1\*</sup>, S. I. Mehtieva<sup>2</sup> and S. Hesarak<sup>3</sup>

<sup>1</sup>Agricultural, Medical and Industrial Research School, Nuclear Science & Tech. Research Institute, Karaj, Iran

<sup>2</sup>Azerbaijan National Academy of Science, Institute of Physics, Baku, Azerbaijan

<sup>3</sup>Biomaterials Lab., Ceramic Dept. of Materials and Energy Research Center (MERC), Tehran, Iran  
fziaie@nrcam.org

### Abstract

Radiation dosimetry was done by measuring free radicals induced in synthetic nano-structure hydroxyapatite (HAP) using EPR method. The HAP samples were synthesized via fluid body simulated method and were irradiated at different dose intervals and subsequently subjected to the EPR measurement. The effects of some EPR parameters were investigated as well. Variations of EPR signal intensities were constructed as peak-to-peak signal amplitude and were compared with alanine and bovine bone samples for two different dose ranges of Gy and kGy from dosimetric point of view. The results were shown that the HAP samples were more practical for doses in Gy range. At kGy range doses the bone sample and alanine dosimeter shows a better EPR responses.

**Keywords:** Radiation dosimetry, nanostructure, hydroxyapatite, EPR.

### Introduction

Electron paramagnetic resonance (EPR) spectroscopy (also known as electron spin resonance, ESR) is an extremely sensitive method for detection and measurement of free radicals. EPR has been widely used in radiation dosimetry, control of irradiated food, polymers, and medical physics. EPR biodosimetry is a physical method based on the measurement of stable radiation induced radicals in the calcified tissues of human body. The individual dose can be best reconstructed using probes that are close to, or part of the exposed individual (Box, 1977). Alanine is relevant to biological dosimetry applications based on the EPR analysis of radiation induced free radicals at high doses. Also some studies have been done about tooth enamel and bone powder for different dose ranges of radiation dosimetry, respectively (Brady *et al.*, 1968; Ziaie *et al.*, 2009). On the other hand, bone and teeth demonstrate the significant variability of dosimetric properties between different samples (IAEA-TECDOC-1331, 2002) and variability in bone is even larger due to higher percentage of organic in its tissue. In addition, sample preparation from these materials often is not so easy. In contrast, the usefulness of enamel and bone for dosimetry results from their high content of hydroxyapatite (Driessens, 1980). Hydroxyapatite (HAP) ( $\text{Ca}_{10}(\text{PO}_4)_6(\text{OH})_2$ ) is a suitable probe for dose reconstruction because it contains stable radiation-induced radicals that are a diagnostic signature of radiation exposure (IAEA-TECDOC-1331, 2002). Therefore, it is anticipated that synthesized HAP can be used for radiation dosimetry purposes. On the other hand process of sample preparation could be effective in the shape of dose-response curve (Oliveira *et al.*, 2000).

In this work, synthetic HAP samples were prepared from fluid body simulated method (Hesarak<sup>3</sup> *et al.*, 2009). The samples were irradiated at different dose intervals

and subsequently subjected to the EPR measurement. The results were compared latter with those of alanine and bovine bone samples for Gy and kGy range doses, from dosimetric point of view.

### Experimental procedure

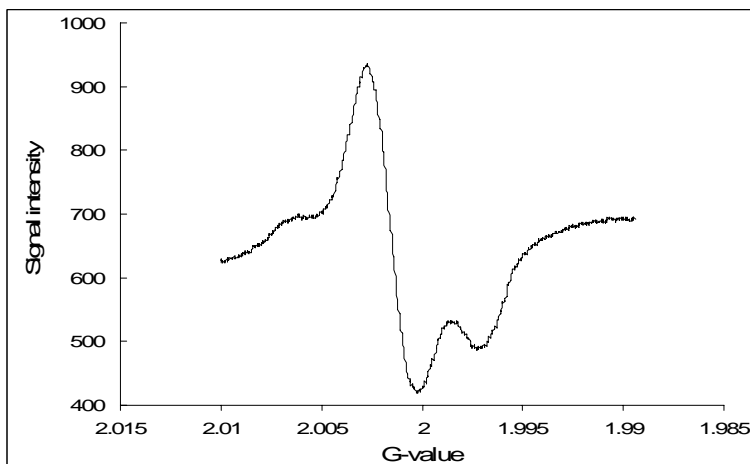
#### Sample preparation

The nano-crystalline HAP was produced utilizing a biomimetic method. The tetra calcium phosphate (TTCP) was produced by heating a mixture of calcium carbonate and decahydrated phosphate anhydrous with 1:1 molar ratio in 1500°C for 6 hours and rapid cooling to room temperature. The resultant product was milled for 6 hour. The mixture of an acidic calcium phosphate, namely brushite, and a basic tetra calcium phosphate was added to a phosphate solution (disodium hydrogen phosphate) at solid to liquid ratio of 3 g/ml and a settable calcium phosphate paste was obtained. The hardened paste was maintained in FBS (Kokubo's solution with ionic concentration similar to that of human plasma) for seven days. At the end of immersion period, the material was removed from the FBS, washed with distilled water, dried at 70 °C, and grinded to a fine powder using a planetary mill (Hesarak<sup>3</sup> *et al.*, 2009). All the used materials were provided from the Merck Company.

#### Microscopic technique

A scanning electron microscope (SEM) XL-30 series, made by Phillips Company, was used to investigate the HAP particle size. The magnification of the system can be obtained using the LaB6 filament ranging from 25x to 400000x. The sample surfaces were coated with a thin gold layer prior to the SEM analysis. Transmission electron microscopy (TEM) system EM208S series was utilized to study and determine the size and morphology of the particles.

Fig. 1. EPR signal of the HAP samples irradiated at 5.61 kGy of dose (Signal intensity in arbitrary units).



#### FTIR analysis

Fourier transmission infrared spectroscopy (FTIR) spectra, was carried out on the samples in the wave number range of 400–4000  $\text{cm}^{-1}$  using a ATI Mattson, Genesis series, made in USA.

#### XRD system

X-ray diffraction (XRD) analysis was performed by a Philips Analytical X-Ray B.V., using Ni-filtered  $\text{CuK}\alpha$  radiation, in the  $2\theta$  range of  $20^\circ$  -  $60^\circ$ .

#### Sample irradiation

The samples were packed in plastic cover and weighted. Irradiation was carried out with two  $^{60}\text{Co}$   $\gamma$ -ray source facilities of PX-30 made in Russia for the kGy range does with the 2.65 kGy/h dose rate and Picker V9 made in USA for the Gy range does with the dose rate of 12.54mGy/ min. The irradiation was done under electronic equilibrium in Plexiglas with approximately 3% of uncertainty. The correction for the decay of  $^{60}\text{Co}$  radionuclide and the subsequent decrease of the dose rate was performed. The samples were irradiated under various dose intervals from 5 Gy to 95 kGy.

#### EPR measurement

The samples were put into quartz thin-wall EPR tubes (4 mm diameter) and measured with a Bruker EMS-104 spectrometer operating in X-band. The EPR signal intensities were measured as peak to peak height for the most intense EPR lines (first derivative of the absorption spectra as shown in Fig.1) per sample mass. In order to ensure the reproducibility of EPR signal intensity, the samples were examined at the

same instrument settings. For each sample, the mean value from four EPR measurements was obtained and the standard deviation of the mean was calculated, which were less than 3% for all measurements. Attempts were made to optimize some of the more important parameters of the EPR system. The microwave frequency is automatically selected by the system. The microwave power is one of the most important parameter among the others. The variation range of this parameter is from 50  $\mu\text{W}$  to 50 mW for the EPR system used. The output EPR signal strongly depends on the sample geometry. The result of the EPR measurement can be affected by the mass, volume and particles size (Ranby & Rabek, 1997). Therefore, one of the most important parameter is the sample height in the EPR tubes and which must be aligned in the EPR cavity. Other parameters used for this study were: 0.285 mT modulation amplitude, 100 kHz modulation frequency, 3.0 mT scan width, 1024-point field resolution, 164 msec time constant, 21 sec sweep time, 50 dB receiver gain, and 4 number of scans.

Fig.2. XRD pattern of the synthesized HAP sample

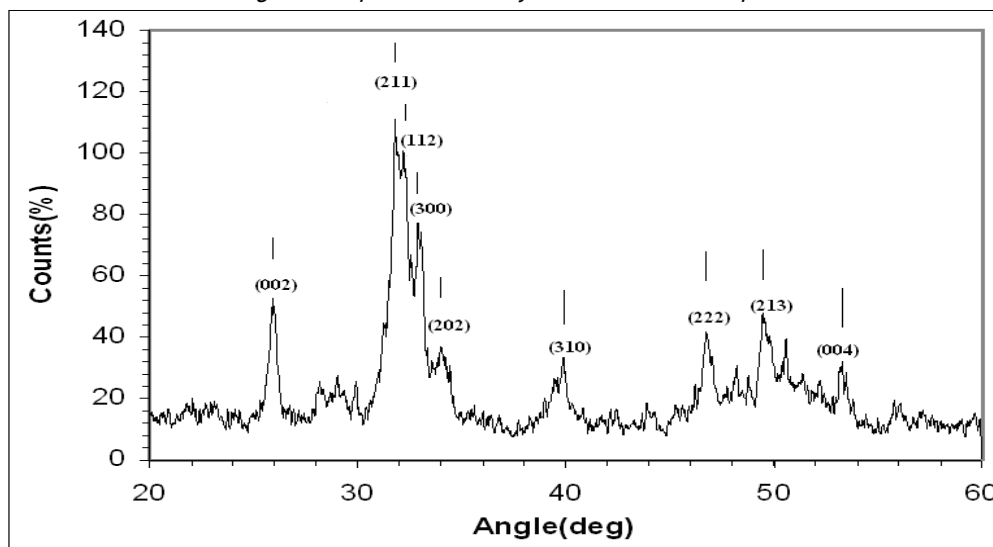
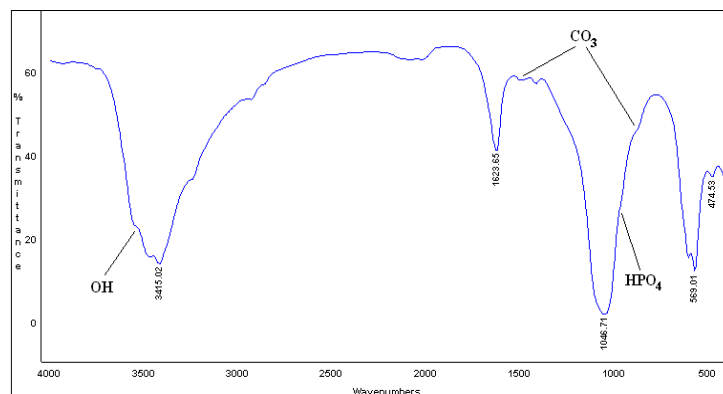


Fig.3. FTIR pattern of the synthesized HAP sample.



## Results and discussion

### HAP characterization

Fig.2 and Fig.3 show the XRD pattern and FTIR spectrum of the HAP powder sample, respectively. All peaks observed in Fig. 2 are related to the apatite phase. The weak peak intensity of the HAP coupled with peak broadening clearly reflects the poor crystallinity (crystallite size/crystal imperfection) of this phase. From the FTIR spectrum analysis, the appeared bands at  $865\text{ cm}^{-1}$  and  $1400\text{-}1500\text{ cm}^{-1}$  are attributed to  $\text{u}_2\text{-CO}_3$  (low C-O region) and  $\text{u}_3\text{-CO}_3$  (high C-O region), respectively, showing carbonate substitution for  $\text{PO}_4$  in apatite lattice (Kweh *et al.*, 2002). The observed band around the  $890\text{ cm}^{-1}$  is referred to  $\text{HPO}_4$  (Ishikawa *et al.*, 1999). Microstructures of the biomimetic HAP nano-crystals are shown in Fig. 4 and Fig .5 using SEM and TEM apparatuses. The results obtained by SEM and TEM apparatus shows the particle size of the HAP sample in range of 25-50nm.

Fig.4. SEM image of the synthesized HAP nano-crystal.

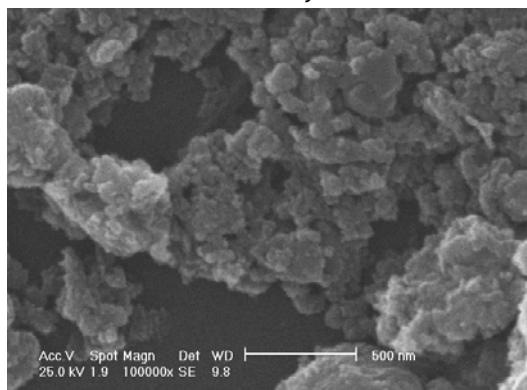
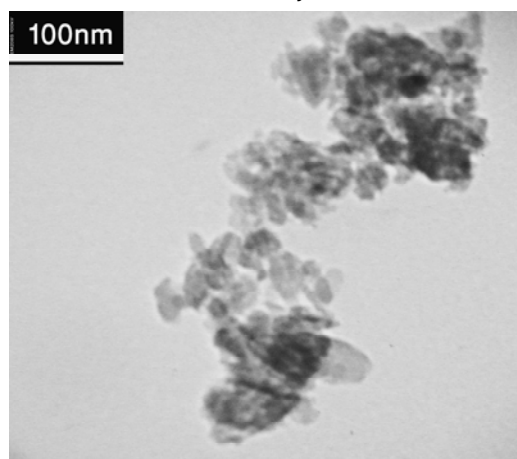


Fig.5. TEM image of the synthesized HAP nano-crystal.



### Effect of microwave power

Measurements of the EPR signal intensities with different microwave power levels for two samples of different height indicate that saturation takes place as shown in

Fig. 6. EPR signal intensity variation against the microwave power for the irradiated HAP samples at different doses with the different sample height.

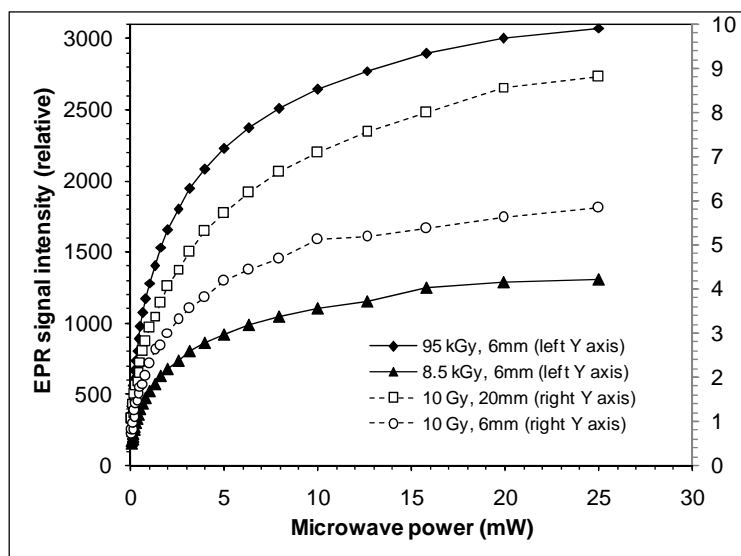


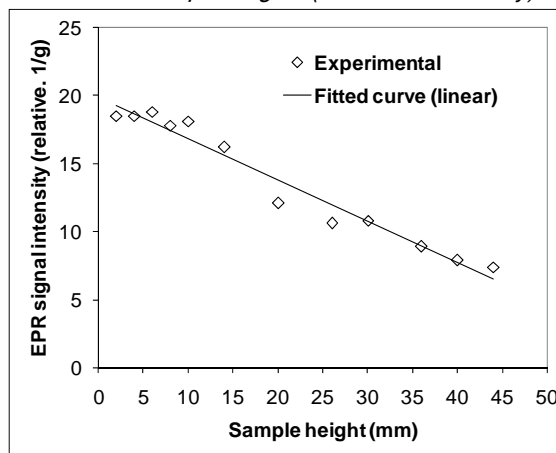
Fig.6 and the value of 15.8 mW was chosen as operating power accordingly (Olsson & Bergstrand, 2001). In addition, it is concluded that this value is independent of the radiation dose.

### Sample height determination

Fig. 6 shows that the EPR signal intensity is higher for the sample height of 20 mm than 6 mm. The effects of sample height on EPR signal intensity variations are shown in Fig.7 and Fig. 8. The EPR responses were mass normalized in Fig.7. In this figure the variations are due to the fact that the microwave intensity and magnetic field are not quite uniform along the EPR system cavity. An increase in sample height increases the microwave phonons absorption at the constant microwave power, and decreases the EPR signal intensity, consequently. Fig. 8 shows that the EPR response is saturated with sample height of nearly 20 mm, as the maximum allowed sample height. In authors view, the sample height and mass could affect the EPR response due to the different effect of non

uniformity of magnetic field and the variety of sample absorbance due to sample density, respectively.

Fig.7. Mass normalized EPR signal intensity variation via HAP sample heights (irradiated at 20 kGy)



### Dosimetric aspects

The entire sample masses were chose less than 100 mg and the sample heights were less than 5 mm.

Fig.9 shows the EPR signal intensity variations as a function of absorbed dose for the HAP samples in comparison with the bovine bone at the Gy range doses.

Fig.8. Non mass normalized EPR signal intensity variation via HAP sample heights (irradiated at 20 kGy)

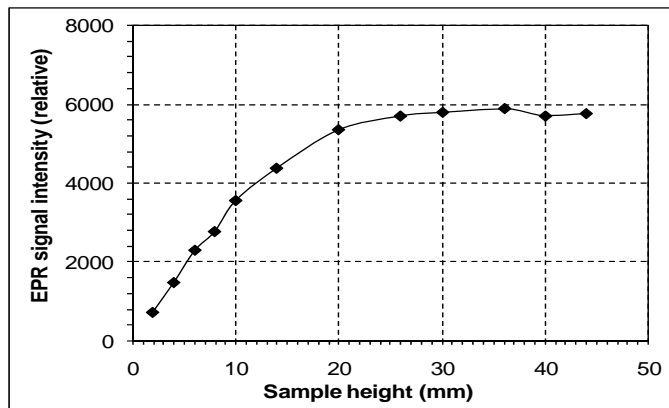


Fig.9. EPR signal intensity variations as a function of absorbed dose for the HAP samples in comparison with the natural bovine bone (low doses).

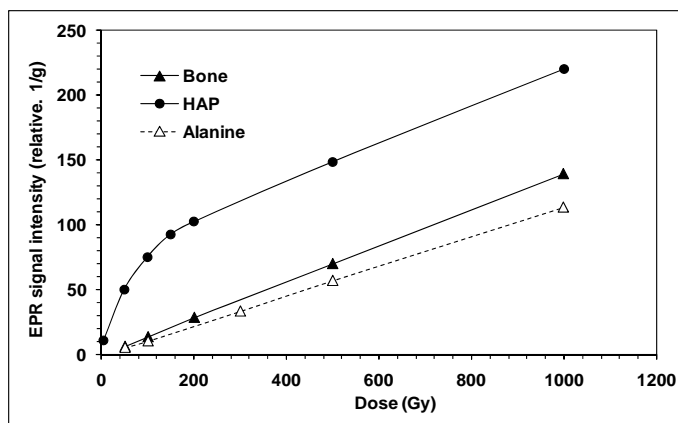
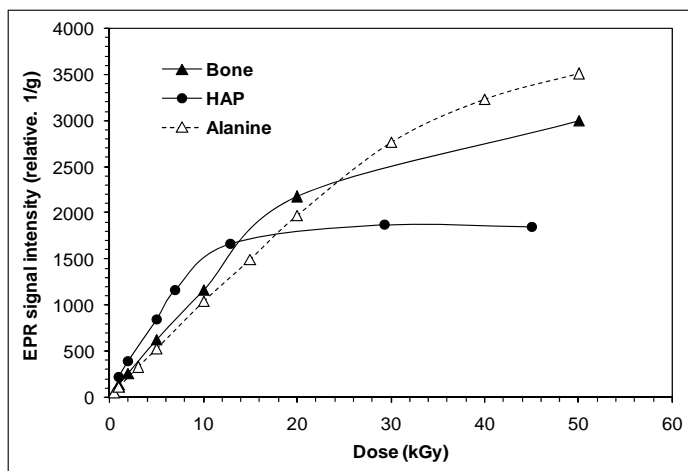


Fig.10. The EPR signal intensity variations as a function of absorbed dose for the HAP samples in comparison with the alanine and bone samples responses for high dose level.



The EPR signal intensity variation of the HAP and bone are almost the same after about 200 Gy and nearly straight line, but the EPR response of HAP is higher than bone. Considering these results it could be concluded that the HAP samples are more practical for the Gy range doses due to the higher EPR intensity in comparison with those of bone samples. Fig.10 shows the EPR response of HAP sample in comparison with alanine dosimeter and bone at high doses (Ziaie *et al.*, 2009). From this figure, the EPR intensity of HAP sample is saturated at about 10 kGy, where the alanine and bone samples are saturated at higher doses.

In the authors view, the carbonate impurities in the HAP sample in comparison with the bone powder is low and not enough to obtain a comparable EPR signal intensities in high doses. But, the induced radical population was enough to results the EPR response with a higher intensity in the Gy range doses. On the other hand, the sample crystal size have important role affecting the EPR response of the samples. The carbonated impurities are incorporated into or attached to the surface of hydroxyapatite crystals during formation, are converted to radicals through absorption of ionizing radiation. The contribution of the radiation induced radicals is mostly due to the attached carbonated impurities on the surface of hydroxyapatite crystals (Moens *et al.*, 1993). Therefore, it was expected that a decrease in hydroxyapatite crystals size, increases the average crystals surfaces and the EPR response, consequently. According to the obtained results using the SEM and TEM microscopes, the particle size of the HAP sample is nano range, where the used bone sample was in micron size. Therefore, the EPR response of the HAP sample is higher in comparison to the other samples at doses less than 10 kGy.

## Conclusion

The value of 15mW is chosen for microwave power to have a good signal observation. This value is almost independent of the absorbed radiation dose. The EPR response is affected by the sample geometry, specially the sample height. It is concluded that the selected sample height in the EPR tube should be less than 20 mm. Comparing the EPR response of the HAP, bovine bone, and alanine dosimeter at the dose range of 1 kGy to 10 kGy show that the HAP is almost linear and higher than alanine and bone but, at higher doses the results are vice versa. Also at the high doses, the EPR response of the HAP is saturated earlier than the others, while at dose range of 5 Gy to 1 kGy the HAP has higher response than bone and alanine. It seems that the bone powder could produce more free radical population at high doses than HAP, due to the higher carbonate impurity. But at the Gy range doses, the carbonate impurity is sufficient for both samples and the obtained differences could be attributed to the particle size. The synthesized HAP is a nano-

crystalline and therefore its EPR signal intensities are higher at the Gy dose range.

### Acknowledgement

The authors wish to acknowledge the kind cooperation of Iran National Science Foundation (INSF).

### References

1. Box HC (1977) Radiation effects: ESR and ENDOR analysis. Academic Press, NY.
2. Brady JM, Aarestad NO and Swarts HM (1968) *In vivo* dosimetry by electron spin resonance spectroscopy. *Med Phys.* 15, 43-47.
3. Driessens FCM (1980) The mineral in bone, dentine and tooth enamel. *Bull. Soc. Chem. Belgrade.* 89, 663-689.
4. Hesaraki S, Moztarzadeh F, Nemati R and Nezafati N (2009) Preparation and characterization of calcium sulfate-biomimetic apatite nanocomposites for controlled release of antibiotics. *J. Biomed. Mater. Res. B (Appl. Biomater).* 91(2), 651-661.
5. IAEA (2002)\_ Use of electron paramagnetic resonance dosimetry with tooth enamel for retrospective dose assessment. Tec. Doc.1331.
6. Ishikawa K, Takagi S, Chow LC and Suzuki K (1999) Reaction of calcium phosphate cements with different amounts of tetracalcium phosphate and dicalcium phosphate anhydrous. *J. Biomed. Mater. Res. A,* 46, 405-510.
7. Kweh SWK, Khor KA and Cheang P (2002) An *in vitro* investigation of plasma sprayed hydroxyapatite (HA) coatings produced with flame-spheroidized feedstock. *Biomaterials.* 23, 775-785.
8. Moens P, Volder PD, Hoogewijs R, Callens F and Verbeeck R (1993) Maximum-likelihood common factor analysis as a powerful tool in decomposing multi component EPR powder spectra. *J. Magn. Reson.* 101, 1-15.
9. Olsson S and Bergstrand ES (2001) Calibration of alanine dosimeters. ISRN. Report 92.
10. Oliveira LM, Rossi AM and Lopes RT (2000) Gamma dose response of synthetic A-type carbonated apatite in comparison with the response of tooth enamel. *Appl. Radiat. & Isot.* 52, 1093-1097.
11. Ranby B and Rabek JF (1997) ESR spectroscopy in polymer research. Springer-Verlog. 38, 4785-4794.
12. Ziaie F, Hajiloo N, Fathollahi H and Mehtieva SI (2009) Bone powder as EPR dosimetry system for electron and gamma radiation. *Nukleonika.* 54 (4), 267-270.